Volume 3 Issue 1 (March 2023)
DOI 10.24191/jaeds.v3i1.62
eISSN 2805-5756

Journal of Applied Engineering Design & Simulation

Separation efficiency analysis of multiphase flow inside hydrocyclone using CFD

M. Mazwan Mahat, Hazran Husain*, Nor Safwan Mohmad
School of Mechanical Engineering, College of Engineering, University Teknologi MARA, 40450 Shah Alam, Selangor, Malaysia
*corresponding author: hazran@uitm.edu.my

ABSTRACT

Separation phenomena inside the hydrocyclone often encounter issues related to misplaced particles at the outlet since there is a large variation of particle density. This research presents a computational numerical study of multiphase flow inside hydrocyclone to analyse the relationship between separation efficiency of particles and the diameter of the cylindrical section to complete the separation process which greatly affect the overall performance of hydrocyclone. The performance of hydrocyclone will be evaluated using CFD to simulate multiphase flow inside the hydrocyclone. In this study, the Reynolds Stress Model (RSM) is used in the model to simulate the swirling turbulent flow of gas and liquid, and the Volume of Fluid (VoF) Multiphase Model is used to simulate the interface between the liquid and the air core. The Discrete Element method (DEM) model simulation of particle flow then makes use of the results to track the solid particle motion. Pressure and velocity play important roles in the separation of particles. A centrifugal force that separates particles according to their mass is produced when the hydrocyclone's input is subjected to higher pressure. The hydrocyclone rotates and produces a spiral flow pattern as the fluid's velocity increases as it goes towards the centre of the device. Higher diameter of the cylindrical section, provide higher tangential velocity of particles and their centrifugal forces, resulting in great collection efficiency. In this paper, it has been demonstrated numerically that the performance of hydrocyclone is significantly influenced by different diameters of the cylindrical sections. Increasing the diameter of the cylindrical section increased the separation efficiency from 34.4% to 44.3% for particle size of 5 μm. Based on the pressure, velocity and streamlines distribution profiles obtained, the results revealed that the tangential velocity contributes largely to the centrifugal forces, resulting in greater collection at the outlet. The increase in diameter increases the residence time of particles inside the hydrocyclone, causing a more frequent swirl rotation of the particles; thus, increasing the clarity of particle separation and enhances the separation efficiency.

Keywords: Multiphase, Hydrocyclone, CFD, Separation Efficiency

Nomenclature

K	Turbulent kinetic energy (J/kg)
$\mathcal{E}$	The Rate of Dissipation of The Turbulent Kinetic Energy

Abbreviations

CAD	Computer aided design
CFD	Computational fluid dynamics
DEM	Discrete element method
FYP	Final year project
LDA	Laser doppler anemometry
LES	Large eddy simulation
LPT	Lagrangian particle tracking
MPPIC	Multiphase particle in cell
RNG	Re-normalisation group
RSM	Reynolds Stress Model
TFM	Two-fluid model
VoF	Volume of fluid

Received on 28.03.2023
Accepted on 11.05.2023
Published on 12.05.2023

1.0 INTRODUCTION

Hydrocyclone is a cyclonic separation device that has ability to separate particle suspensions based on particle size, density, and shape. Hydrocyclone utilizes a centrifugal force generated from the flow of liquid that enters the cyclone tangentially at high speed which helps to create a liquid vortex in the cyclone [1]. Slurry liquid contained a mixture of substances that enter through tangential inlet as shown in Figure 1 will separate according to the specific gravity of the particles and in addition to their size. The bottom of the chamber features a restricted axial bottom outlet via which none of the liquid in the vortex can escape known as underflow or spigot. Some of the liquid must flow in the opposite direction and counter currently to an axial top outlet called overflow or vortex finder. Due to the lower pressure along the axis of rotation, this reverse flow continues to rotate, forming an air core.

To analyse the performance of a hydrocyclone, engineers use various mathematical models to experiment the hydrocyclones' potential. The application of numerical methods such as Computational Fluid Dynamics (CFD) to model the performance of hydrocyclone is one of main assessment tools that is widely used.

Previous studies have proved CFD to be a reliable tool of predicting the internal flow field of a hydrocyclone [2-4]. There are various parameters affect the performance of hydrocyclones. It is important to optimize the cyclone design based on particle flow and vortex flow patterns to improve the separation the particle efficiency of multiphase substances [5].

Although hydrocyclone is widely used at present in various application such as oil and gas industry and mineral processing industry, the study of the separation phenomena inside the hydrocyclone are still being proposed until today.

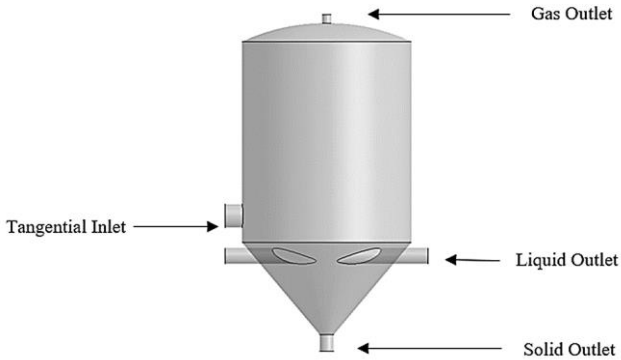

Figure 1. Schematic representation of a hydrocyclone

2.0 METHODOLOGY

2.1 Geometric modelling of hydrocyclone

There are four designs of three-phase hydrocyclones used in this study in order to study the separation efficiency based on different sizes of cylindrical section diameter. The base of the geometric modelling used in all four designs are the same, except the cylindrical section diameter. The geometric was designed as a CAD model in CATIA V5R21 software as shown in Figure 2 according to the dimensions provided in Table 1. Next, the model was exported to ANSYS design modeler as solid and later converted to volume to study the interphase of the fluid. The geometrical parameters and dimensions mentioned were taken from the previous study to offer a reliable comparison.

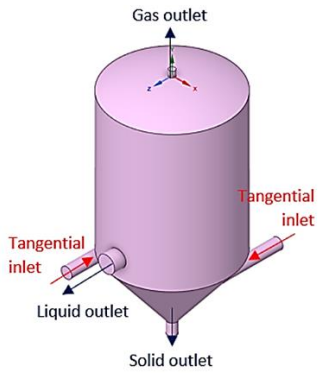

Figure 2. Geometrical model of three-phase hydrocyclone

Table 1: Geometrical details of designed hydrocyclone

Dimensions	Value
Diameter of the tangetial inlet [mm]	200
Diameter of the solid outlet [mm]	150
Diameter of the gas outlet [mm]	100
Diameter of the liquid outlet [mm]	300
Cylindrical section diameter [mm]	Type (A) 1200 Type (B) 1600 Type (C) 2000 Type (D) 2400
Height of the cylindrical section [mm]	2500
Included cone angle	53°

2.2 Numerical simulation setup

The use of Computational Fluids Dynamic software in this study is based on conservation laws of physics which are mass, momentum and energy conservations. This software adequately predicts the flow of fluids and related phenomena in the fluid region of interest by numerically solving the mathematical equations (1 - 4),

Conservation of mass

$$\frac{\partial \rho}{\partial t} + \frac{\partial}{\partial x}(\rho u) + \frac{\partial}{\partial y}(\rho v) + \frac{\partial}{\partial z}(\rho w) = 0 \tag{1}$$

where,

ρ = density
u, v, w= components of velocity
x, y, z = direction of velocity

Equation (1) illustrates the partial differential form of continuity equation for conservation of mass which indicates that the rate of change of mass within the control volume is equivalent to the mass flux crossing the volume surface. In order to perform simulation, this equation requires relevant inputs such as boundary conditions and initial parameters.

Conservation of momentum

For x-direction (U-momentum)

$$\rho\left(\frac{\partial u}{\partial t} + u\frac{\partial u}{\partial x} + v\frac{\partial u}{\partial y} + w\frac{\partial u}{\partial z}\right) = -\frac{\partial P}{\partial x} + \frac{\partial}{\partial x}\left[2\mu\frac{\partial U}{\partial x} - \frac{2}{3}\mu\left(\frac{\partial u}{\partial x} + \frac{\partial v}{\partial y} + \frac{\partial w}{\partial z}\right)\right] + \frac{\partial}{\partial y}\left[\mu\left(\frac{\partial u}{\partial y} + \frac{\partial v}{\partial x}\right)\right] + \frac{\partial}{\partial z}\left[\mu\left(\frac{\partial u}{\partial z} + \frac{\partial w}{\partial x}\right)\right] + \rho g_x \tag{2}$$

For y-direction (V-momentum)

$$\rho\left(\frac{\partial v}{\partial t} + u\frac{\partial v}{\partial x} + v\frac{\partial v}{\partial y} + w\frac{\partial v}{\partial z}\right) = -\frac{\partial P}{\partial y} + \frac{\partial}{\partial x}\left[\mu\left(\frac{\partial v}{\partial x} + \frac{\partial u}{\partial y}\right)\right] + \frac{\partial}{\partial y}\left[2\mu\frac{\partial v}{\partial y} - \frac{2}{3}\mu\left(\frac{\partial u}{\partial x} + \frac{\partial v}{\partial y} + \frac{\partial w}{\partial z}\right)\right] + \frac{\partial}{\partial z}\left[\mu\left(\frac{\partial v}{\partial z} + \frac{\partial w}{\partial y}\right)\right] + \rho g_y \tag{3}$$

For z-direction (W-momentum)

$$\rho\left(\frac{\partial w}{\partial t} + u\frac{\partial w}{\partial x} + v\frac{\partial w}{\partial y} + w\frac{\partial w}{\partial z}\right) = -\frac{\partial P}{\partial z} + \frac{\partial}{\partial x}\left[\mu\left(\frac{\partial w}{\partial x} + \frac{\partial u}{\partial z}\right)\right] + \frac{\partial}{\partial y}\left[\mu\left(\frac{\partial w}{\partial y} + \frac{\partial v}{\partial z}\right)\right] + \frac{\partial}{\partial z}\left[2\mu\frac{\partial w}{\partial z} - \frac{2}{3}\mu\left(\frac{\partial u}{\partial x} + \frac{\partial v}{\partial y} + \frac{\partial w}{\partial z}\right)\right] + \rho g_z \tag{4}$$

where for equations (2) to (4),

P = static pressure
μ = dynamic viscosity of a fluid
ρ = density
ρg_x , ρg_y , ρg_z = body forces in the x, y and z directions
u, v, w= components of velocity
x, y, z = direction of velocity

Due to the complexity hydrocyclone's swirling flow movement, the modelling process is divided into three steps as shown in Figure 3.

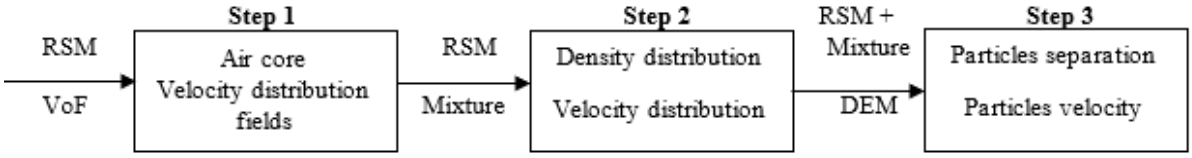

Figure 3. Schematic Simulation Modelling used in Present Study

In step 1, the flow of liquid and gas phases are considered. The presence of anisotropic in the air flow was modelled using Reynolds Stress Model (RSM), since the RSM method is able to capture the flow dynamics of hydrocyclone accurately. This model has proved to be an optimum turbulence model choice compared to the RNG k-ε method based on the previous studies [6,7] where it accurately predicted the velocity profiles with the best estimation in water split ratio. Large eddy simulation (LES) is another method that is suitable in solving the turbulence model problems. However, it is much more suitable for a large size hydrocyclone, and needs much higher number of computational mesh compared to RSM method.Then, the volume of fluid (VoF) model is used to illustrate the free interface between air core and liquid. This stage allows for the acquisition of the primary air core position and velocity distribution. VoF used continuity equation to track the location of the free surface in detail. It is often the model of choice due to the presence of more than two immersible fluids [8,9].

In step 2, the results obtained in the first step were used to describe the behaviour of magnetite particles with different sizes. The VoF model is changed to mixture approach. The result of density and velocity distribution in this step were utilized as the initial conditions for the third step. The solid particles are modelled using Discrete Element Method (DEM). This method has proved to accurately track particle motion at high feed solids concentrations compared to Lagrangian particle tracking (LPT) method as mentioned in a past study [10]. Here, the sand particles are added and the flows of solid, liquid and gas through the outlet are examined in order to measure the hydrocyclone separation efficiency. Hence, the whole process involves three CFD models which are RSM, VoF, and DEM as outlined in Figure 3.

In the general setup, the pressure-based setting was chosen, and the velocity formulation was set to absolute. Steady time and gravitational acceleration were set to z-axis in the negative direction to indicate that the gravitational forces act on the opposite direction of the geometrical modelling. The first setting that must be taken into account is the multiphase flow since this study deals with two different flows of fluids which are liquid and gas. The volume of fluid (VoF) model was used to illustrate the free interface between air core and liquid by utilizing the continuity equation to track the location of the free surface in detail. As mentioned earlier, this study used the Reynolds Stress Model (RSM) to present the anisotropic of the air flow inside the hydrocyclone. Standard wall functions and model constants were set to default setting. Since this research focuses on the separation efficiency, the discrete phase was turned on to set up the injection properties. Surface injection type was selected as the injection will inject solid particles over the tangential inlet surface. The injection will have the same speed as the entering fluid, which is at 2.469 m/s. The injection is initialized using face normal direction and uniform diameter distribution, at a total flowrate of 0.0001 kg/s. The three phase substance in this study are mixtures of crude oil (liquid), natural gas (gas) and sand (solid). Table 2 provides the information of the physical characteristics of the mixture.

Table 2: Physical properties of crude oil, natural gas and sand mixture

Parameter	Value
Density (crude oil)	830 kg/m^3
Viscosity (crude oil)	2.0 Pa.s
Density (natural gas)	0.717 kg/m^3
Viscosity (natural gas)	0.003 Pa.s
Density (sand)	2650 kg/m^3
Uniform diameter of sand	5μm

The cell zone condition was set as mixture type for the multiphase flow and the operating conditions for pressure was set to atmospheric at 101325 Pa. The boundary conditions of stationary wall motion and no slip condition were applied to the hydrocyclone walls. The velocity inlet boundary was applied at the tangential inlet and the pressure outlet at all the outlets including solid, liquid and gas outlet. The volume fraction of fluid liquid to gas was set to 0.4. The discrete phase type for walls and tangential were set to ensure the continuous flow of

stream inside the hydrocyclone. Escape discrete phase type was applied at liquid and gas outlet indicate that the particles will escape through the exit channel. In order to track the solid particles, trap type discrete phase was set at the solid outlet for final separation efficiency analysis. The SIMPLE scheme algorithm was implemented in the solutions methods and the second order upwind were utilized for other control equations. In solution initialization, standard method was applied and computed from the tangential inlet of the hydrocyclone.

2.3 Verification

In order to obtain the highest accuracy and reliable results, it is essential to make verification in terms of numerical modelling and parameters used in CFD software. There are very few literature that performed the study of three-phase hydrocyclone experimentally and through simulation. Verification of numerical modelling needs a legit literature that performed on-site measurements before conducted a simulation. Referring to the mentioned limitations, the numerical modelling is verified with previous research by Farah Miza et al. [11] and Khairy Elsayed et al. [12]. To validate this simulation results, the tangential velocity profile and axial velocity profile at y position (designated as H2 as shown in Figure 4) were computed and compared with the results from mentioned references.

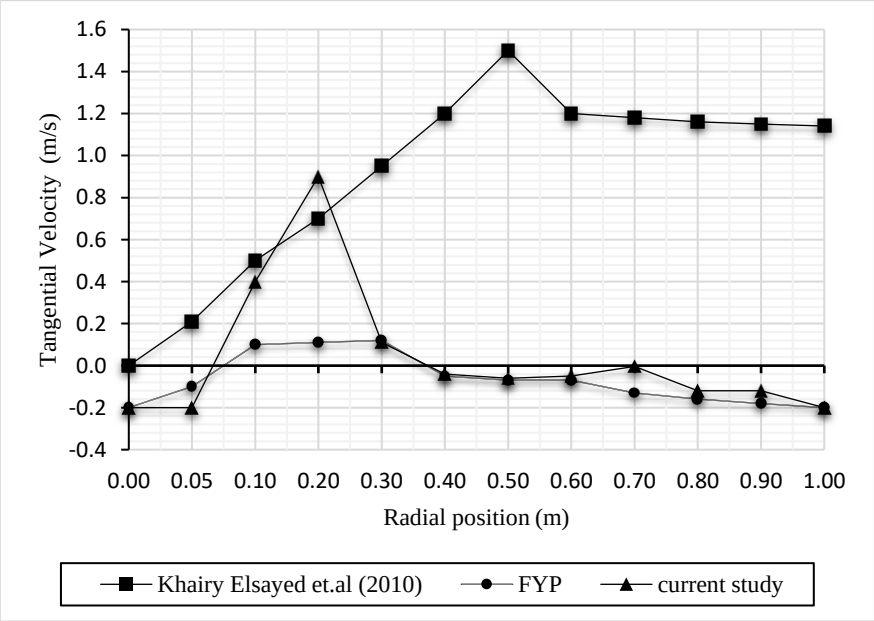

Figure 4. Comparison Tangential Velocity Distribution Between Previous Study (FYP) and Current Research

The tangential velocity obtained are compared in Figure 4. The current study follows a similar trend to Farah Miza et al. [11] (labelled as FYP) and Khairy Elsayed et al. [12]. The tangential velocity starts to increase gradually before descending after a certain radial position. Since this study used various different parameters compared to previous study except the geometrical model, the trend is not exactly identical to the previous research. The trend still shows a good agreement between the current simulation and previous studies in comparison with the tangential velocity. The results have the same tendency as the results from both previous studies, although quantitatively they are different.

3.0 RESULTS AND DISCUSSION

3.1 Pressure Distribution profiles

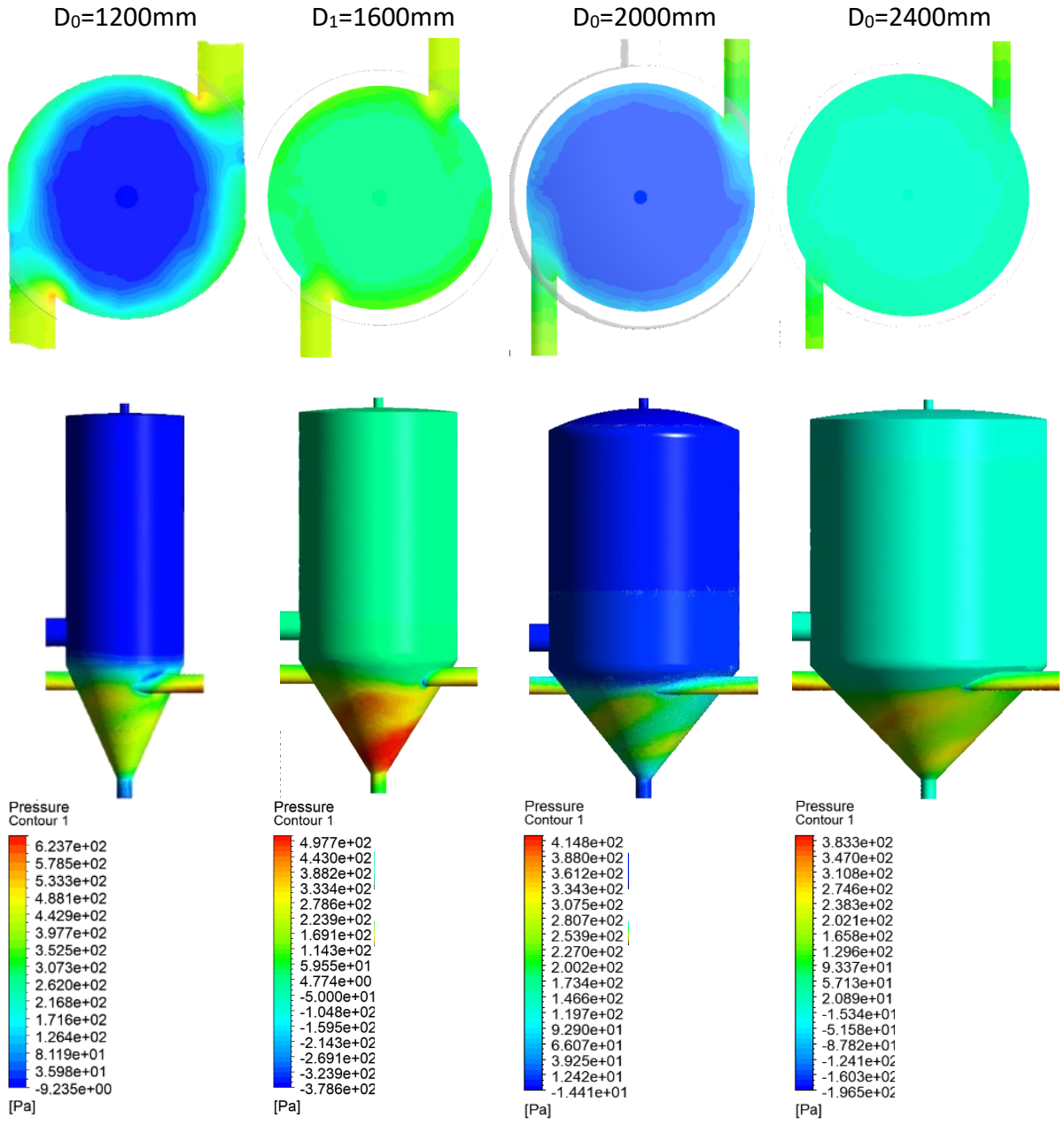

Figure 5. Pressure Distribution Profiles with Cylindrical Section Diameter of (a) 1200mm, (b) 1600mm, (c) 2000mm, (d) 2400mm

This study simulated the effect of different sizes of cylindrical section diameter on the overall separation efficiency at constant inlet flow rate of a three-phase mixture. The pressure distribution in the hydrocyclone is shown in Figure 5. The average pressure dropped radially as the mixture moves from the wall to the centre. A negative pressure zone gradually forms in the core outflow areas of the hydrocyclone, changing the pressure inside the cavity. A similar behaviour can be observed in traditional two phase hydrocyclones from previous studies in Refs. [12,13]. The mixture flows through the overflow and underflow outlet due to this area of negative pressure. The profiles also indicate that the highest pressure is concentrated at the conical section due to the collision of fluid streams when the mixture enters tangentially at both inlets. The trend of the highest-pressure value goes down with the increase in cylindrical section diameter from 1200 mm to 2400 mm. To understand more about the pressure distribution, Figure 6 illustrate the pressure distribution based on several radial sizes of the hydrocyclone.

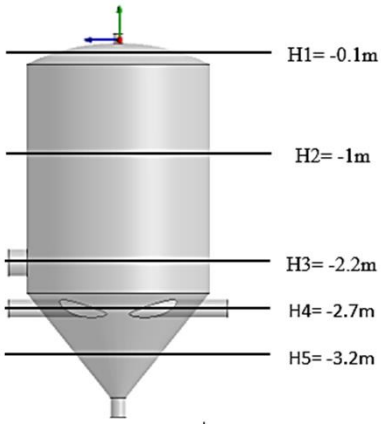

Reference height for the analysis

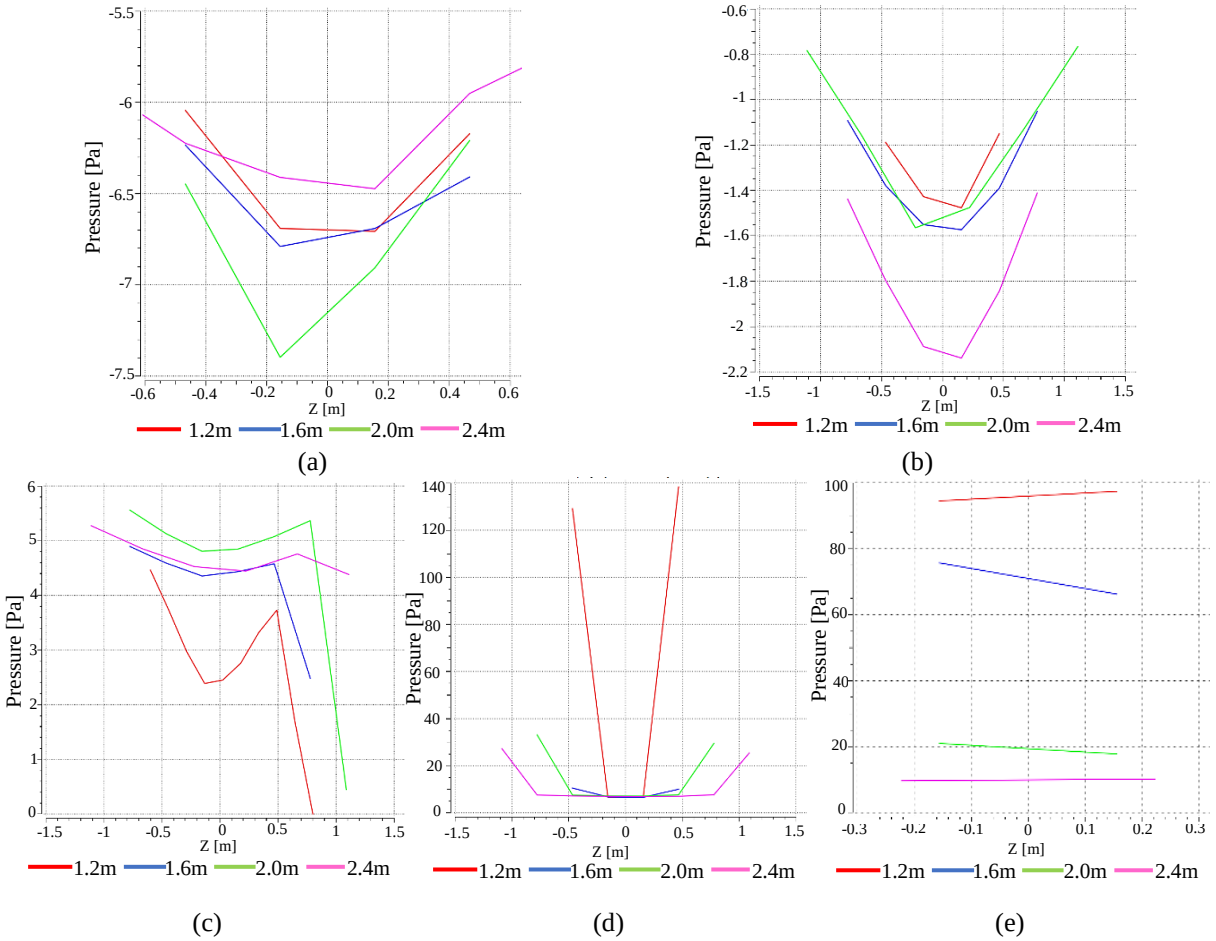

Figure 6. Reference cylinder height and the radial pressure distribution profiles heights of (a) H1, (b) H2, (c) H3, (d) H4, (e) H5

The pressure distribution in Figure 6 were plotted based on the radial position. All four hydrocyclones static pressure readings demonstrate that the pressure reduced from the sidewall towards the core region and is almost centrosymmetrically distributed. As a result, the core component exhibits a negative pressure zone. This follows the general law of the static pressure distribution of the hydrocyclone and is the same as the static pressure distribution law of a conventional hydrocyclone. At the inlet region, Figure 6 (d), a similar trend show the increase in pressure starting from the sidewall towards the inner section of the hydrocyclone. At a larger diameter, the mixture requires to travel much further which explained the lower pressure at the sidewall compared to smaller diameter hydrocyclone. At the liquid outlet , Figure 6 (c) the higher pressure shifted towards the left side region

because there is an outlet located at the left side. The pressure at the outlet increase as the behaviour of the speed pass through outlet decreases.

3.2 Velocity distribution profiles

There are three dimensional components of velocity field inside hydrocyclone which consist of axial, radial and tangential velocity. The internal flow field affects the hydrocyclone separation characteristics, which in turn affect its separation mechanism. The fundamental assumption behind separation is the centrifugal force generated by the tangential velocity. In contrast to how the radial velocity affects the stability of the flow field in the hydrocyclone, the axial velocity establishes the space for separation [14]. The streamline of four different velocity fields is shown in Figure 7 starting from diameter 1200mm to 2400mm. The velocity gradient was relatively uniform for all types of hydricycylone and show a spirally upward decreasing trend. Since the inlet of the four model is located at the upper part of the conical section, the velocity streamlines are maximum in this area due to the incoming accelerated fluid flow. Then as the fluid flow move upwards into the conical section area, the velocity gradually decrease as shown in blue light colour. In Figure 7 (a), the internal swirl formed is concentrated at the centre of the hydrocyclone. As the diameter increases, the swirl formed in the upper part of the hydrocyclone was strengthened. Velocity distribution shifted more towards the outer walls as the diameter of the conical section increased.

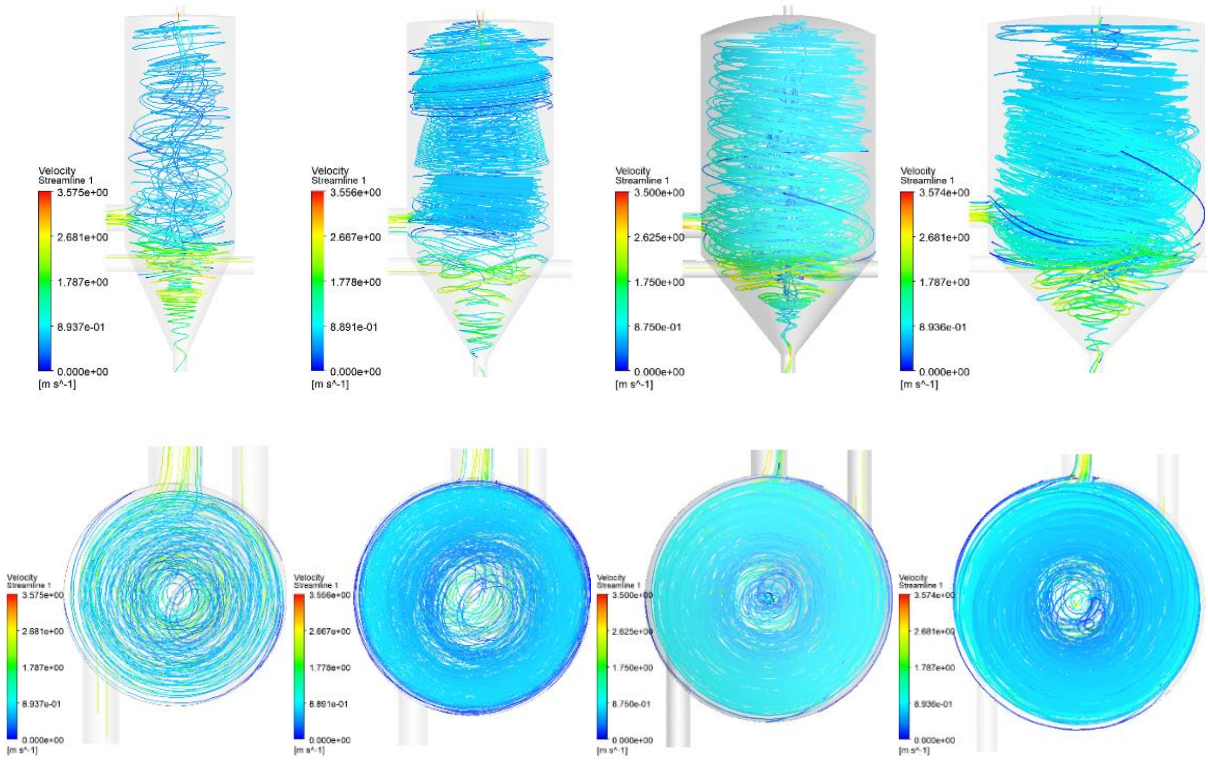

(a) (b) (c) (d)

Figure 7. Front View and Top View Streamlines Profiles Based on Different Cylindrical Diameter Section (a) 1200mm, (b) 1600mm, (c) 2000mm, (d) 2400mm

The streamline profile of the mixture under steady-state flow for different cyclone diameters is shown in Figure 7. At the diameter of 1200 mm, the streamlines quickly shifted towards the centre of the hydrocyclone. In contrast for larger diameters, the fluid swirl strength is greater in the outer region before migrating to the centre of the hydrocyclone. It can be concluded that in the velocity distribution profile, because of the accelerated fluid flow, velocity streamlines are at their highest near the inlet section and the swirl velocity progressively diminish as they ascend to hydrocyclone's upper part before migrating to the centre to descend to the underflow part.

3.3 Axial velocity

The speed at which the fluid swirls or spirals as it enters the cyclone has an effect on the velocity distribution inside the hydrocyclone. The velocity profiles present in the various hydrocyclone types were investigated. The axial velocity profile with different cylindrical section diameter captured at various axial sites, is shown in Figure 9. Standard two phase hyrocyclone with a single entrance hydrocyclone is distinguished by asymmetric profiles, particularly at the entry [15], and advances downhill. The fluid entering from only one side of the vertical axis is the cause of this behaviour. In the twin inlet hydrocyclone like in the present study, the opposite situation can be

seen. The symmetrical axial velocity is provided by the two tangential inlets which produce symmetrical axial velocity profiles with the highest points centred at the centre of the cylindrical structure. The axial velocity contour demonstrate that the type of arrangement prevents the reversing flow from wavering along the core. Similar flow behaviours were observed while several different parameters of cylindrical section diameter. Figure 8 used to clearly illustrate the intensity of the axial velocity. To make a point, the axial location at position H2 in conical section, z = -1m, was selected. The peak velocity uniformly distributed across the cyclone axis for all types of hydrocyclone. The upward movement of reverse flow are more efficient at higher the axial velocity.

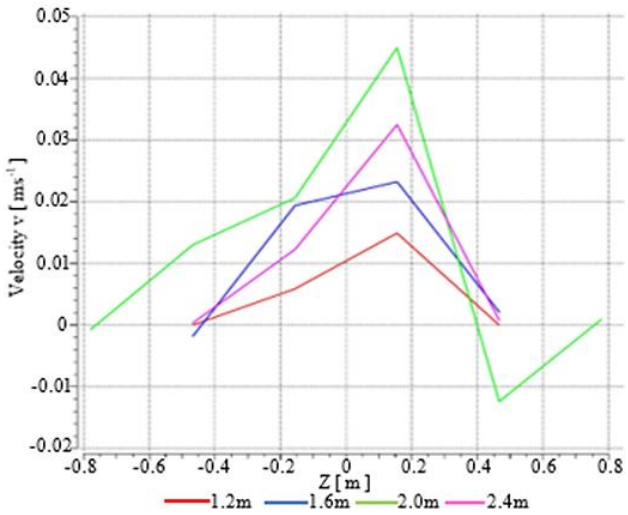

Figure 8. Axial velocity distribution at position H2

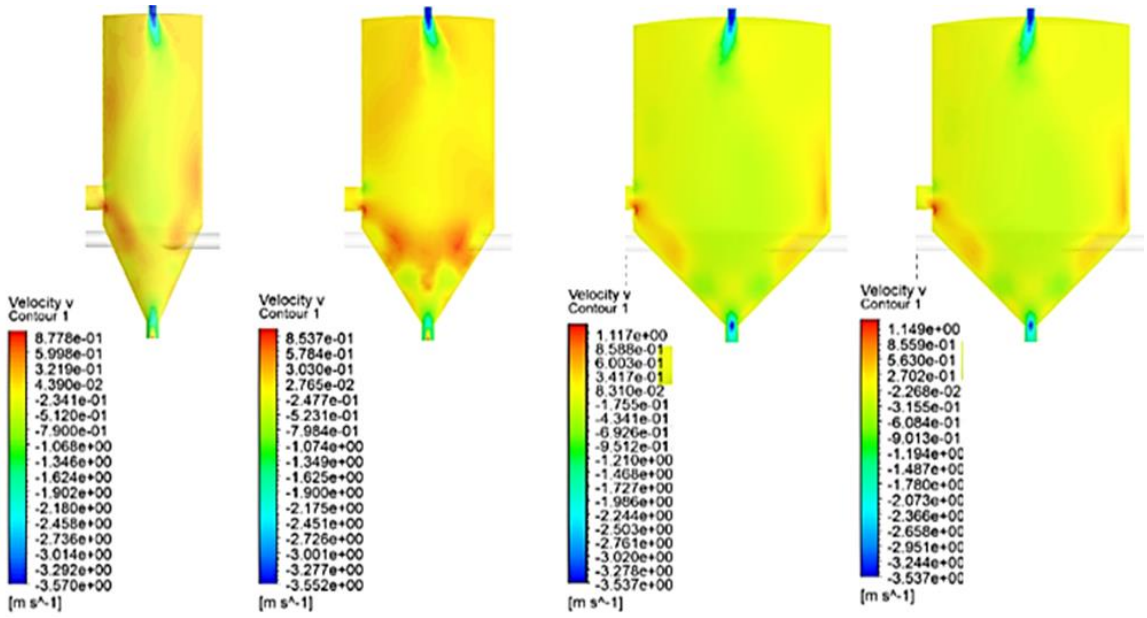

Figure 9. Axial velocity profiles with cylindrical section diameter of (a) 1200mm, (b) 1600mm, (c) 2000mm, (d) 2400mm

3.4 Tangential velocity

It has been demonstrated experimentally that the tangential velocity is a combination of a forced vortex close to the hydrocyclone axis and free vortex in the outer wall region by ignoring the impact of the wall boundary layer. The centrifugal forces required to separate the fluid based on density differences are influenced by the fluid swirling movement, which is influenced by the tangential velocity. Their widths were determined by the distribution of swirl intensity along the cyclone's axis. Figure 10 shows the tangential velocity distribution along the y-z plane. In the centre region of the hydrocyclone structure, the tangential velocity has the lowest value. The

swirl intensity has led the tangential velocities to increase from the cyclone's axis to a height after which they decrease to zero at the walls. The tangential velocity clearly demonstrates increasing in trend as the radial distance radius increases. In dual inlet cyclone exhibits nearly symmetrical velocities across the investigated axial regions. Left side region and right region have almost similar value of axial velocity despite negative value indicate the opposite direction from the inlet. From the results, a higher diameter cylindrical section shows greater tangential velocity magnitude than smaller diameter cylindrical section which means type (d) hydrocyclone has greater swirl potential compared to other design.

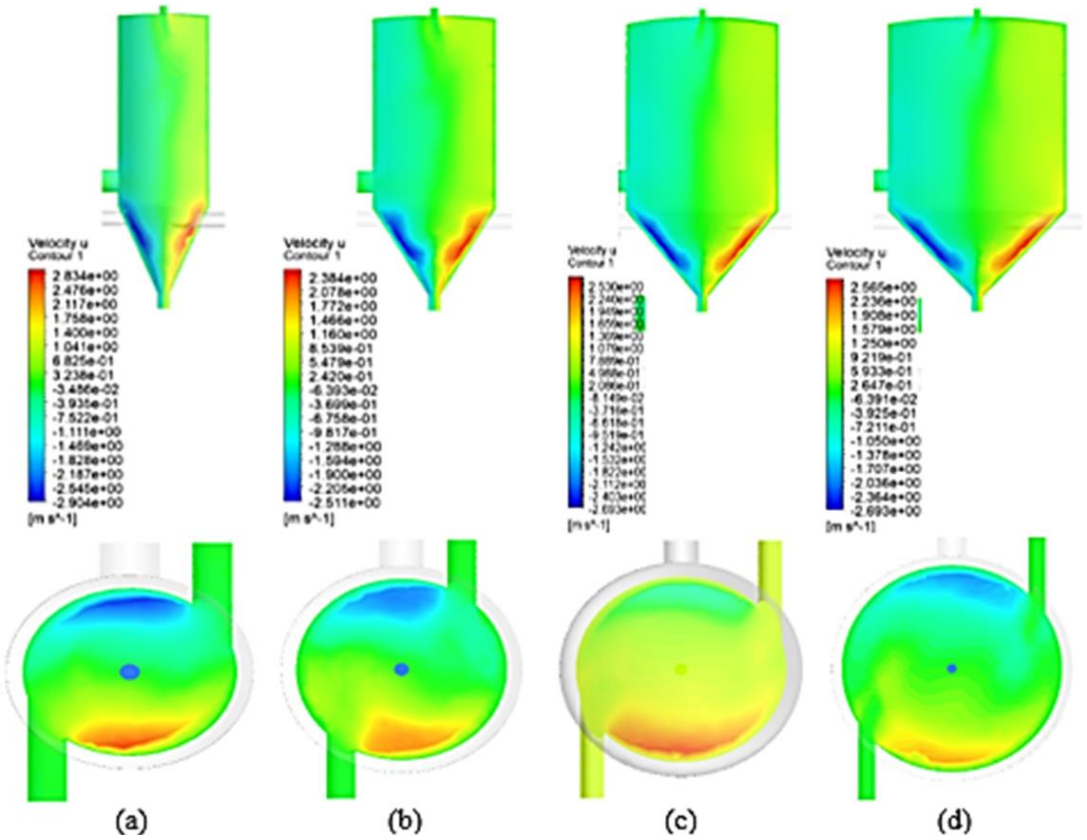

Figure 10. Tangential velocity with cylindrical section diameter of (a) 1200mm, (b) 1600mm, (c) 2000mm, (d) 2400mm

3.5 Radial velocity

Figure 11 demonstrate the radial velocity distribution inside the three phase hydrocyclone. As can be seen from the top view of the hydrocyclone, the distribution of the radial velocity in all four types of hydrocyclones have two side of different value at inlets, positive on one side and negative at the other side. This is due to the symmetrical shape of the hydrocyclone where identical inlets were present at both side of the hydrocyclone. Overall, the simulation result of radial velocity presents a symmetrically distributed pattern at cylindrical sections of the hydrocyclone.

In the hydrocyclone's initial stage, the radial velocity was distributed with high symmetry from the inlet. In Figure 11 (a), (b), (c) and (d), general pattern of radial velocity was predicted as the velocities are all directed towards the axial centre from the wall starting at the inlet. The highest radial velocity present in the region near the inlet and then increases steadily as the radius shrinks before abruptly decreasing after reaching its maximum value close to the axial centre, which is consistent with the radial velocity distribution of the sink flow. The liquid outlet also shows a higher value of radial velocity due to the collision between the fluid particles swirling inside the hydrocyclone. When passing through the small area led in increasing in axial velocity which explained the higher value at the gas and the liquid outlet. The high positive radial velocity at the centre aids in the rapid exit of the low-density phase from the hydrocyclone and increases the low-density phase's separation effectiveness for example gas form.

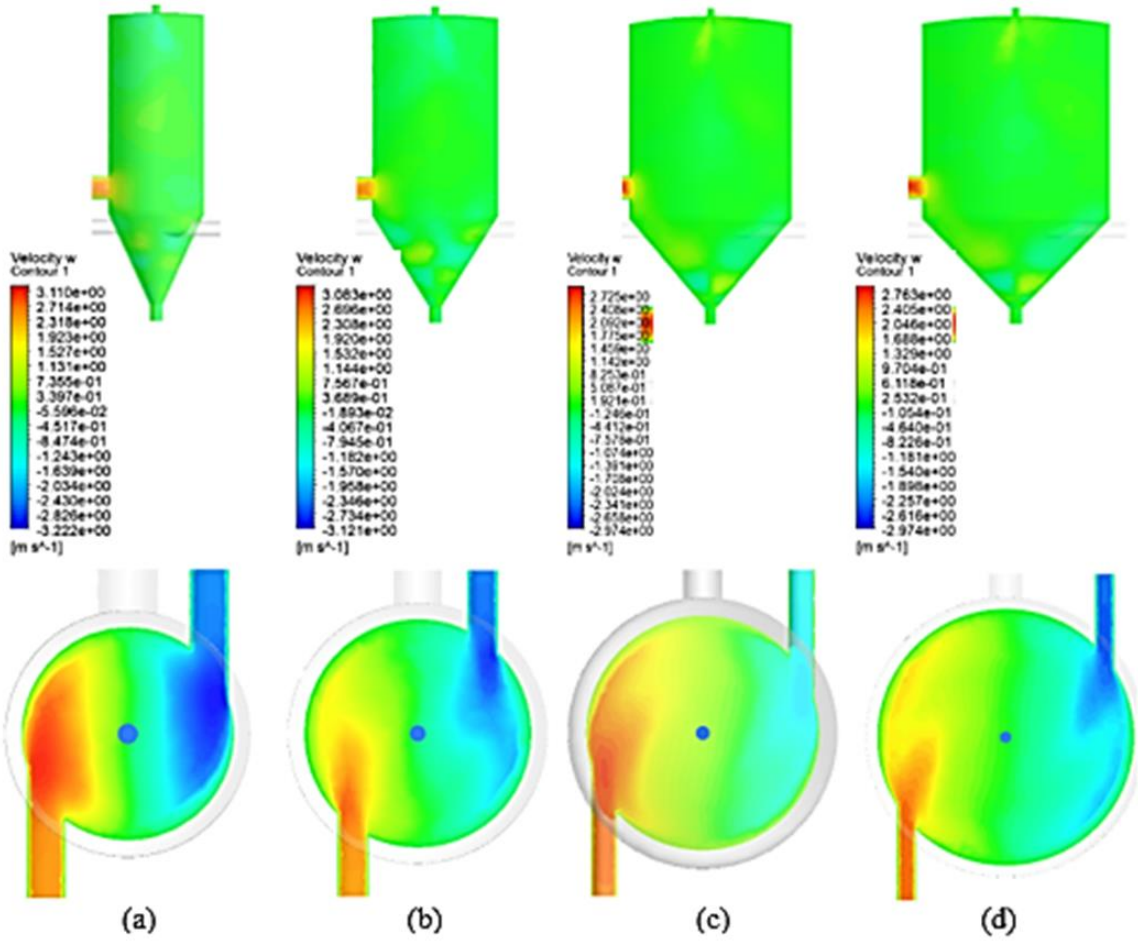

Figure 11. Radial Velocity with Cylindrical Section Diameter of (a) 1200mm, (b) 1600mm, (c) 2000mm, (d) 2400mm

3.6 Discrete Phase

Typical particle trajectories collected into the underflow (solid outlet) are shown in Figure 12 in order to identify differences between particle trajectories at different hydrocyclone diameters. Because a modest variation in particle size has less of an impact on the calculation of the flow field, sand particles with a diameter of 5μm were used. Volumetric flow rate of solid particles in experiments and simulations is 3%.

The diameter of sand particles in mixture phase can be regarded as discrete phase due to its very small particle size. Therefore, in this study, the solid particles were tracked and calculated using the DPM model. When particles are injected into the hydrocyclone, the centrifugal effect causes the particles to move rotationally and migrate toward the hydrocyclone wall. After a few revolutions, the particles in type (a) hydrocyclone insdicate that the particles swiftly flow into the upper part of the hydrocyclone. In type (b) hydrocyclone, the rotation of the particles occurred more frequently before shifting its flow path towards the upper section. Because of the greater centrifugal force brought on by the higher fluid velocity, type (d) particles rotate more frequently compared to others. Type (d) experienced the highest number of rotations. Particles spend more time in the column section which increases the residence time, which then increased number of rotations they undergo, resulting in increases the effect of clarity separation and boosts separation accuracy and efficiency. This is due to the fact that in the cylindrical region, a fairly symmetrical and high velocity distribution are developed, resulting in a prolonged particle residence period.

The separation effect primarily influences the principal forces acting on the solid particles in the hydrocyclone, including the centrifugal inertial force, centripetal buoyancy, and fluid resistance. The driving force behind centrifugal separation is the centrifugal inertial force. As mentioned earlier, the tangential velocity has great impact on the centrifugal inertial force. Due to the symmetrical high-speed fluid injection, the tangential inertial force of the type D hydrocyclone is stronger than those of the other three hydrocyclones at the same radial position. Greater tangential velocity translates to the discrete phase experiencing increased centrifugal force.

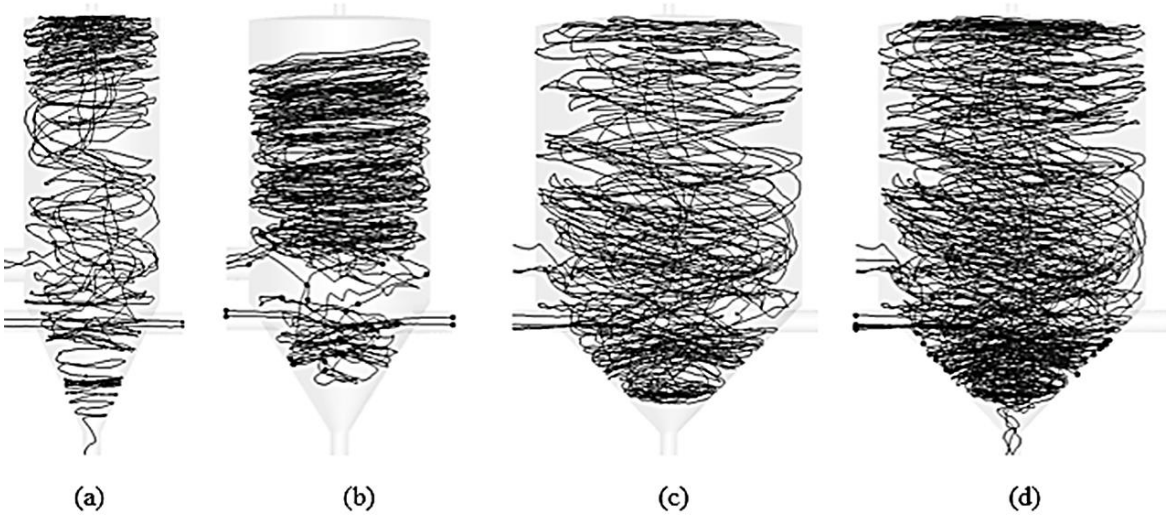

Figure 12. Particle motion trajectory for different diameters of hydrocyclone, at (a) 1200mm, (b) 1600mm, (c) 2000mm, (d) 2400mm

3.6 Separation efficiency

An essential metric for assessing the effectiveness of the hydrocyclone is separation efficiency. In order to calculate the collection efficiency, this study used the same formula suggested by Prachi [2, 4]. The ratio of the number of particles collected in the underflow stream to the number of particles in the feed stream were calculated to provide a detail behaviour of individual particles in the hydrocyclone. The results obtained were used in determining the separation efficiency of the hydrocyclone. Since the sand particles were injected through the inlet surface, ANSYS tracks all the particles that enters and leaves the system. From the information, the separation efficiency can be calculated to determine which setup provide the best performance for separating sand particles.

The experiment was conducted at the same total flow rate of 0.001kg/s and scaled by face area in order to examine the categorization performance of the type (A), (B), (C) and (D). The diameter distribution of sand particles was set to uniform at 5μm and was injected using face normal direction. The result of the DPM iteration from all type of hydrocyclone is shown in Table 3. The number of particles tracked are in the range of between 3780 to 4140. Note that for Type A and Type D, there were particles that had an incomplete trajectory. Particles that had an incomplete trajectory were caught in the flow. As a result, the particles were unable to reach the outlet within the time steps specified in this simulation. However, by raising the time step count won't be able to address all the particles to complete their trajectory because certain particles will always be trapped inside the flow. As a result, this study has chosen the statistical threshold, such that 92% of the particles must exit the domain, to judge whether the discrete phase is sufficiently simulated.

Table 3: The result of discrete phase for different types of hydrocyclone

	Type A-1200mm	**Type B-1600mm**	**Type C-2000mm**	**Type D-2400mm**
Particles tracked	3960	3840	4140	3780
Particles escaped	2518	2351	2493	1936
Particle trapped	1319	1489	1647	1540
Incomplete	123	0	0	304

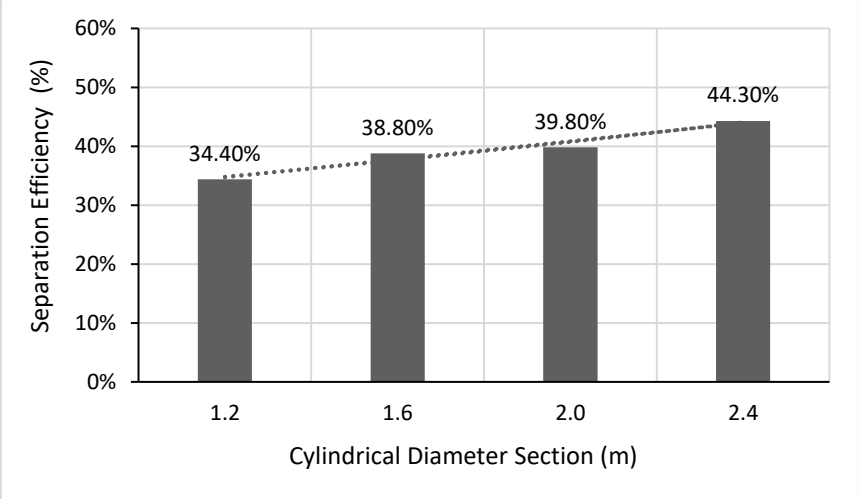

Figure 13. Separation efficiency on different cylindrical diameter

As seen in Figure 13, an increase in diameter of the cylindrical section leads to higher solid particle separation efficiency for all tested three-phase hydrocyclone. Increasing the diameter of the cylindrical section by 1200 mm boost almost 10% of separation efficiency. Hydrocyclone with cylindrical section diameter of 1200 mm obtained the lowest efficiency at 34.40%. By increasing the cylindrical section diameter to 1600 mm, increase the efficiency by 4.4%. A slight different in trend occur from 1600 mm to 2000 mm, where minor increase in efficiency of 1% was displayed. Lastly, increasing to 2400 mm cylindrical diameter lead to efficiency of 44.30%. Major increase in efficiency at this range for about 4.5%. Overall, the graph show rising trend in separation efficiency as the cylindrical diameter section of the hydrocyclone increased.

Since all the parameters and geometrical models were kept constant except for the cylindrical section diameter, it can be concluded that the results obtained are dependent on the only variable that changes. The velocity distribution is higher in larger cylindrical section diameters, resulting in higher efficiency compared to smaller size cylindrical section diameter. Furthermore, longer particle residence time also contribute to higher separation efficiency. Additionally, since the model of the hydrocyclone used two tangential inlets, it worth noting that it largely contribute to the increase in tangential velocity of particles and their centrifugal forces, resulting in great collection efficiency.

3.6 Separation efficiency two phase hydrocyclone and three phase hydrocyclone

In the industrial setting, hydrocyclones are frequently employed for liquid-liquid or liquid-solid separation. Two phases can be separated using a two-phase hydrocyclone, whereas three phases can be separated using a three-phase hydrocyclone. The separation of a two-phase hydrocyclone is based on the disparity in densities of the two immiscible liquids. While the lighter liquid is pulled to the centre of the hydrocyclone and leaves through the overflow, the heavier liquid is forced to the outer wall of the hydrocyclone. The density and viscosity of the fluids, the flow rate, and the size and geometry of the hydrocyclone are the primary determinants of separation efficiency. While in a three-phase hydrocyclone are separated based on their relative densities and interfacial tensions. The higher density liquid is forced to the outer wall, while the lower density gas is forced to the inner section. Centrifugal force and fluid drag work together in a hydrocyclone to separate solid particles from a liquid stream by producing swirling flow pattern which cause the solid particles to move in the direction of the hydrocyclone outer wall down to underflow outlet.

Wang and Yu [8] presented a numerical analysis of the multiphase flow of gas, liquid, and solid in hydrocyclones with various body construction parameters, including the lengths of the conical parts diameters. In this paper, scale factors ranging from 0.25 to 3 (body diameter from 18.75 to 225 mm correspondingly) are used as shown in Table 4. A similar pattern to the current study can be observed in Figure 14. As the separation efficiency increases as body diameter increases at a given inlet velocity. These results could be explained from the changes to the orbit radius of particles. As the body diameter increases, the orbit radius increases. Consequently, the probability for particles to move to the wall of the body and then move down with the downward flow is decreased. For a particle diameter of 5 μm (indicated in red line), the separation efficiency ranges from 15% to 30%. Similar to the current study using three-phase hydrocyclone, the influence of the diameter increase to the separation efficiency is evident although the geometrical modelling is different.

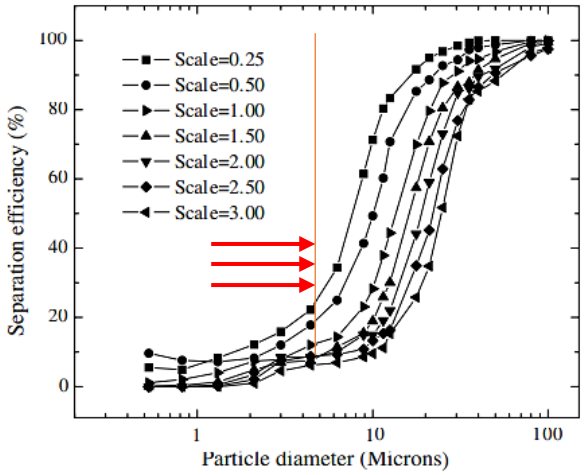

Figure 14. Separation efficiency varies with particle diameter [8]

Table 4: Values of the changing variables for simulation

Parameter	Symbol	Dimension (mm)				
Diameter of the body	D_c	18.75	37.5	112.5	150	187.5
Length of cylindrical part	L_c	25	50	100	125	150
Length of conical part	L_p	35	85	135	235	285

4.0 CONCLUSION

This study primarily examines the separation efficiency in three-phase hydrocyclone and the separation efficiency based on four different hydrocyclone parameters. The geometrical models were subjected to simulations having the same parameters except for four variations in the diameter of the cylindrical section, ranging from 1200 mm to 2400 mm. It has been demonstrated numerically that the performance of a hydrocyclone is significantly influenced by the cylinder diameter. Increasing the diameter of the cylindrical section increased the separation efficiency from 34.4% to 44.3% for a particle size of 5 µm. A 30% increase in the cylindrical section diameter from 1200 mm to 1600 mm led to an increase in the separation efficiency by 4.4%. However, a slight difference in trend occur from 1600 mm to 2000 mm, where a minor increase in efficiency of 1% was displayed. Then, increasing to 2400 mm cylindrical diameter again led to a high improvement in separation efficiency by 4.5%.

Based on the pressure, velocity and streamlines distribution profiles, the tangential velocity contributes largely to the centrifugal forces, resulting in great collection. The velocity distribution are higher in much larger cylindrical section diameter resulting in higher efficiency compared to smaller size cylindrical section diameter. Furthermore, longer particle residence time also contribute to higher separation efficiency. Additionally, since the model of the hydrocyclone used two tangential inlet, it is worth noting that it largely contribute to the increase in tangential velocity of particles and their centrifugal forces, resulting in greater collection efficiency.

REFERENCES

[1] Akhbarifar S., Shirvani M., Zahedi S., Zahiri M.R., Shamsaii Y.," Improving Cyclone Efficiency by Recycle and Jet Impingement Streams," Iranian Journal of Chemistry and Chemical Engineering (IJCCE), 30(2): 119-124, 2011.

[2] Sonali Swain, Swati Mohanty, "A 3-dimensional Eulerian–Eulerian CFD simulation of a hydrocyclone," Applied Mathematical Modelling 37(5), 2921-2932, 2013.

[3] Vega-Garcia, D., Brito-Parada, P. R., & Cilliers, J. J., "Optimising small hydrocyclone design using 3D printing and CFD simulations," Chemical Engineering Journal, 350, 653–659, 2018.

[4] Izadi, M., Makvand, A. M., Assareh, E., & Parvaz, F., "Optimizing the design and performance of solid–liquid separators," International Journal of Thermofluids 100033, 5–6, 2020.

[5] Tongsir, S., "The Simulation of Hydrocyclone Network for Separating Yeast and Calcium in Ethanol Production, in Chemical and Process Engineering", King Mongkut's University of Technology North Bangkok, 2007.

[6] Rudolf, P., "Simulation of multiphase flow in hydrocyclone," *EPJ Web of Conferences, 45*, 2013.

[7] Brennan, M.S., Narasimha, M., Holtham, P.N, "Multiphase modelling of hydrocyclones–prediction of cut-size," Miner. Eng. 20, 395–406, 2007.

[8] Wang, B., Yu, A.B., "Numerical study of particle–fluid flow in hydrocycloneswith different body dimensions," Miner. Eng. 19 (10), 1022–1033, 2006.
[9] Mousavian, S.M., Najafi, A.F., "Numerical simulations of gas–liquid–solid flowsin a hydrocyclone separator," Archive of Applied Mechanics 79 (5), 395–409, 2009.
[10] Narasimha, M., Brennan, M., Holtham, P.N., "A review of CFD modelling for performance predicitons of hydrocyclone.," Engineering Applications of Computational Fluid Mechanics 1 (2), 109–125, 2007.
[11] Farah Miza, "Computational Fluid Dynamics Study On Vortixx Compact Flotation Unit," Faculty of Mechanical Engineering Universiti Teknologi MARA (UiTM). [Accessed Feb 31, 2022]
[12] Khairy Elsayed , Chris Lacor, "Optimization of the cyclone separator geometry for minimum pressure drop using mathematical models and CFD simulations," Chemical Engineering Science, 65(22),:6048-6058, 2010.
[13] Zhou, Cuihong & Wang, Shihan & Yang, Changshun & Xu, Ling., "Study on Particle-Size Control of Hydrocyclone for Slurry Recycles," *IOP Conference Series: Earth and Environmental Science*, 2018.
[14] Zhao, Z., Wang, H., Xie, C. et al, "Hydrocyclone separation performance influenced by feeding solid concentration and correcting separation size," Heat Mass Transfer 57, 63–76, 2021.
[15] Nunes S, Magalhães H, Neto S et al., "Impact of permeable membrane on the hydrocyclone separation performance for oily water treatment," Membranes 10, 350, 2020.